RF magnetron-sputtered coatings deposited from biphasic calcium phosphate targets for biomedical implant applications

K.A. Prosolov [a, b, *], K.S. Popova [a], O.A. Belyavskaya [a], J.V. Rau [c], K.A. Gross [d], A. Ubelis [e], Yu.P. Sharkeev [a, b]

[a] Institute of Strength Physics and Materials Science of SB RAS, Tomsk, Academicheskii pr., 2/4, 634055, Russia
[b] National Research Tomsk Polytechnic University, Tomsk, Lenina pr., 30, 634050, Russia
[c] Istituto di Struttura della Materia, Consiglio Nazionale delle Ricerche (ISM-CNR), via del Fosso del Cavaliere 100, 00133, Roma, Italy
[d] Faculty of Materials Science and Applied Chemistry, Riga Technical University, Azenes Str. 14/24, Riga, LV-1048, Latvia
[e] University of Latvia, 19, Raina blvd., Riga, LV-1586, Latvia

ARTICLE INFO

ABSTRACT

Bioactive calcium phosphate coatings were deposited by radio-frequency magnetron sputtering from biphasic targets of hydroxyapatite and tricalcium phosphate, sintered at different mass % ratios. According to Raman scattering and X-ray diffraction data, the deposited hydroxyapatite coatings have a disordered structure. High-temperature treatment of the coatings in air leads to a transformation of the quasi-amorphous structure into a crystalline one. A correlation has been observed between the increase in the Ca content in the coatings and a subsequent decrease in Ca in the biphasic targets after a series of deposition processes. It was proposed that the addition of tricalcium phosphate to the targets would led to a finer coating's surface topography with the average size of 78 nm for the structural elements.
© 2017 The Authors. Production and hosting by Elsevier B.V. on behalf of KeAi Communications Co., Ltd. This is an open access article under the CC BY-NC-ND license (http://creativecommons.org/licenses/by-nc-nd/4.0/).

1. Introduction

In the field of the regenerative medicine, the bioactivity of the implants is strongly associated with an interlayer between the bone and the implant. One of the widely used materials for implants is titanium (Ti) which has a naturally occurring titanium oxide (TiO_2) coating on its surface. This TiO_2 interlayer makes Ti biocompatible. However, in order to improve implant stability and provide osseointegration, calcium phosphate (CaP) bioactive coatings are used. According to the accepted classification of bioactive materials with respect to the criteria for the apatite formation mechanism, the first bioactive materials group includes Hydroxyapatite (HA) and β-Tricalcium phosphate (TCP) [1]. CaP has gained much

attention as a possible material to be used in regenerative medicine due to its ability to form and support bone growth on its surface. This property is called osseoconductivity. In addition, bioactivity and biodegradation are important features of CaP. The difference of various CaP biodegradation rate is mainly related to the chemical composition of the material and the level of osseoconductivity. The HA, TCP and biphasic ceramics (BPC) have different levels of the osseoconductivity in vivo, which is inversely proportional to the rate of bio-resorption [2,3]. The lowest bio-resorption rate of the HA can be used to produce long-term stability coatings in comparison with other CaPs. Moreover, compared to TCP, the HA is more closely related to the mineral component of the bone marrow. On the other hand, the bioactivity of the TCP is much higher than that of HA due to its rapid dissolution and bio-integration [4].

Due to the poor mechanical properties, defects arise during the use of implants composed solely of CaP. As a result, the CaP materials are mostly used as coatings on metallic implants. Such composites possess good mechanical properties due to the metallic base and increased level of osseointegration due to the CaP coating. This plays an important role in the development of new composite types as implant performance is largely affected by the properties

---

* Corresponding author. Institute of Strength Physics and Materials Science of SB RAS, Tomsk, Academicheskii pr., 2/4, 634055, Russia.
E-mail addresses: konstprosolov@gmail.com (K.A. Prosolov), popova@ispms.tsc.ru (K.S. Popova), obel@ispms.tsc.ru (O.A. Belyavskaya), giulietta.rau@ism.cnr.it (J.V. Rau), karlis-agris.gross@rtu.lv (K.A. Gross), arnolds@latnet.lv (A. Ubelis), sharkeev@ispms.tsc.ru (Yu.P. Sharkeev).
Peer review under responsibility of KeAi Communications Co., Ltd.

of the coating material of the implant.

Several reports have been published on the formation and properties of thin radio-frequency (RF) magnetron sputtered coatings of different CaP compositions. HA [5–7] and TCP [8–10] coatings are the most widely studied CaP deposited materials for biomedical applications. Less frequent studies involve tetracalcium phosphate [8,10], calcium pyrophosphate [11,12] and calcium metaphosphate [10]. The interest in thin RF magnetron deposited calcium phosphates is connected to the high adhesion of the coatings to the substrate. It is possible to control the elemental composition of coatings by sintering the sputtering targets from homogeneous mixtures of phosphates. The RF magnetron sputtering provides high purity coatings, whose elemental composition is close to that of the sputtering target [13]. It is important to notice that there is a limited number of studies related to deposition of thin bioactive coatings by RF magnetron sputtering of biphasic targets [6,14].

One of the main advantages of biphasic calcium phosphates is their biodegradation rate that can be modified by changing the proportional ratio of the composition phases [15]. Moreover, biphasic calcium phosphate ceramics, namely the hydroxyapatite/β-tricalcium phosphate of the 60% HA/40% TCP composition (in weight %), has been shown to induce bone formation in large, long bone defects [16]. Thus, it is important to work towards deeper understanding and possible applications of biphasic calcium phosphate coatings.

This work aims to propose the possibility of manipulating the structure and the elemental composition of coatings by variation of composition of biphasic targets.

2. Materials and methods

Commercially pure titanium samples (99.58 Ti, 0.12 O, 0.18 Fe, 0.07 C, 0.04 N, 0.01 H wt. %) of the $10 \times 10 \times 1$ mm^3 size were used as substrates. The samples were polished in series using silicon–carbide paper of 120, 480, 600, 1200 grit. Prior to deposition, the samples were cleaned in an ultrasound bath of distilled water for 10 min.

The targets for magnetron sputtering were fabricated and sintered from powders of HA, TCP and their homogeneous mixture. In the case of biphasic targets, the concentrations of HA and TCP were as follows: 75%HA/25%TCP, 50%HA/50%TCP, 25%HA/75%TCP (all in mass %). Hence, five targets were prepared including the targets of pure HA and TCP further denoted as 100HA, 75HA/25TCP, 50HA/50TCP, 25HA/75TCP and 100TCP. The HA powder used for target sintering was manufactured by mechanochemical activation [17]. The TCP powder was purchased from the Budenheim chemical factory (Budenheim, Germany). Press-powder was made from a mixture of initial powder and polyvinyl alcohol.

The targets were manufactured by uniaxial pressing at room temperature by the MIS-6000.4K hydraulic press (Armavir, Russia) in the form of 3–6 mm thick discs of 120 mm diameter. The pressure was changed stepwise 3–4 times. The sintering of the targets was done in the ITM 12.1200 chamber furnace (Tomsk, Russia). A specific sintering mode was applied in accordance with the results of simultaneous thermal analysis of the HA and TCP powders on the STA 409 PCLuxx (NETZSCH-Geratebau GmbH, Germany), which combined differential thermal analysis and thermogravimetry. These results indicated that the sintering temperature needed to be raised to 1000 °C. As a result, the heating and cooling to sinter each target took up to a day and a half.

Deposition of CaP on a Ti substrate was performed by RF magnetron sputtering. A vacuum installation, with a planar magnetron, was utilized and operated at 13.56 MHz along with a closed electron drift ion source (TPU, Tomsk, Russia). Prior to deposition, the surface of each substrate was activated and cleaned by Ar ions for 15 min. This ion cleaning was carried out at an energy level of 1.5–3.0 keV, a current of 10–30 mA and a chamber pressure of 1 Pa. The coatings were prepared by magnetron sputtering at RF-power level of 250 W in an Ar atmosphere. The deposition time was 3 h, and the target-to-substrate distance was 80 mm. During the coating deposition, the working pressure in the vacuum chamber was 0.7 Pa. Each set of samples was deposited in a single run. The average thickness of the coatings, as measured by a Calotest (CSEM Instruments), was 200 ± 15 nm. Investigation of the phase composition was done by a D8 Advance Bruker (Germany) X-ray diffractometer. The XRD experiments were carried out using the Bragg-Brentano geometry with Cu Kα_1 radiation at the angles of $2\theta = 5–60°$ and scanning by steps of 0.01°. The small-angle grazing incidence XRD (GIXRD) with an angle of 0.5° allowed more precise phase composition data from the thin coatings on Ti substrates. Prior to XRD, the samples were annealed in air at 700°C for 1 h to change the structure of coatings from the quasi-amorphous to the crystalline state.

A Raman spectroscopy was carried out using a Renishaw inVia Raman microscope (UK). The laser wavelength in the experiment was 633 nm. Morphology of the coatings was studied with atomic-force-microscopy (AFM) at room temperature by a Solver HV atomic force microscope (NT-MDT, Russia). The elemental composition of each target's zone erosion and that of the coatings was determined by a Philips SEM 515 SEM with an EDAX ECON IV (USA) micro-analyser.

3. Results and discussion

AFM images of the surface topographies of the as-deposited CaP coatings are presented in Fig. 1. The mean average structural elements size was 535 ± 45 nm (Fig. 1a) and was determined by the intercept method from AFM images. Nuclei of new structural elements can be observed on the top of each globular-like structures. Agglomerates of larger size can be, possibly, formed with the growth of overall thickness of the coating. The increase in the concentration of TCP in the biphasic targets leads to the formation of smaller surface features on the coatings' surfaces (Fig. 1b–d). The correlation between the structural elements size in the coatings and the content of TCP in the biphasic targets is presented in Fig. 1f. The addition of TCP to the biphasic targets reduces the size of the surface structures of coatings from 535 ± 45 nm down to 78 ± 19 nm. The smallest size of structures, 28 nm, is related to the case of sputtering a pure TCP target (with the average element size of 78 ± 19 nm, close to the size of biological HA crystallites (30–50 nm) [18]). It should be noted that crystallites in the biological HA are formed as plate-like structures instead of the globular shape topography of our deposited coatings. On the other hand, the attachment and differentiation of osteoblasts are enhanced on more complex, micro-rough CaP surfaces rather than on smooth topographies [19]. Thus, it is possible to manipulate the coating's topography by increasing the concentration of HA or of TCP in the biphasic targets.

Diffraction patterns of as-deposited CaP coatings and of coatings after annealing, obtained in the standard Bregg-Brentano geometry, are presented in Fig. 2. For the as-deposited coatings (Fig. 2a), the high intensity peaks, attributed to the Ti substrate, are registered. The XRD patterns of CaP coatings after treatment at 700 °C for 1 h (Fig. 2b) show peaks of TiO$_2$ (rutile) that appeared after annealing. It is possible to distinguish an expanded peak of small intensity at $2\theta = 31–34°$, possibly belonging to HA. Diffraction intensity of the HA peak is very weak due to the small coating's thickness. The rest of the diffraction peaks are related to the substrate. The same situation was observed for all other types
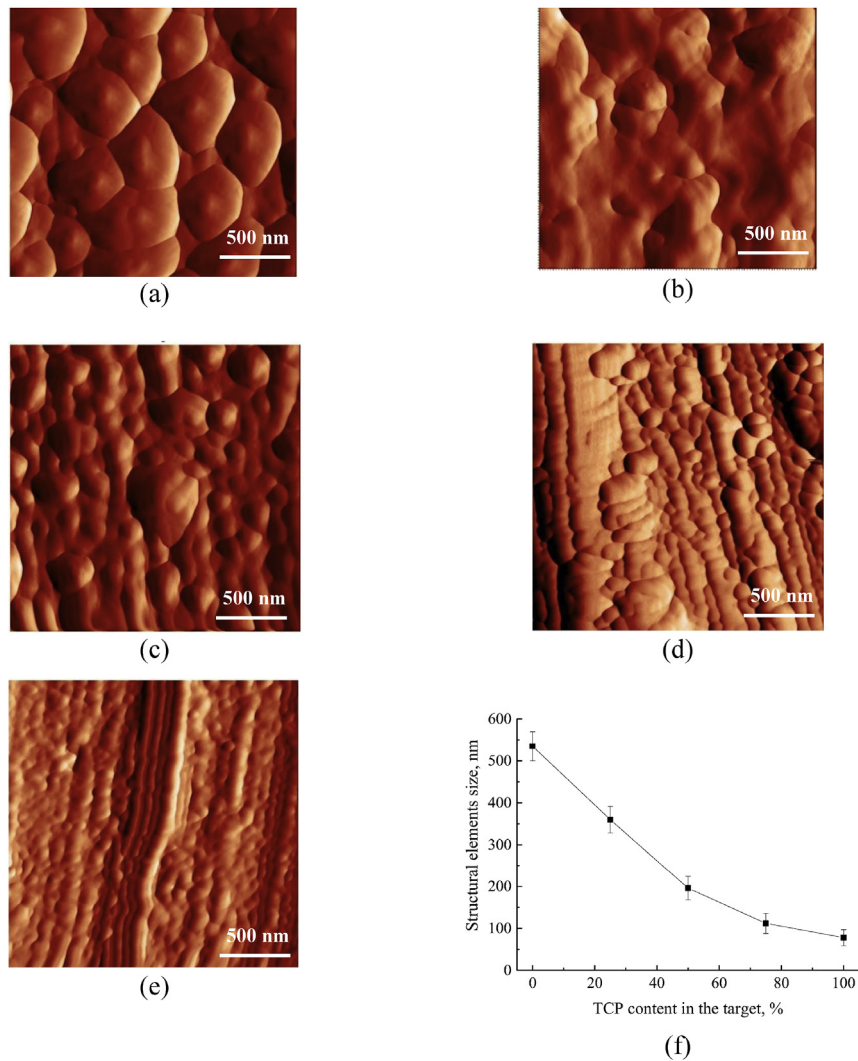
Fig. 1. The morphology of the coatings deposited from the following targets: 100HA (a), 75HA/25TCP (b), 50HA/50TCP (c), 25HA/75TCP (d) и 100TCP (e). Correlation between structural elements size and TCP content in the target (f).

of coatings.

The GIXRD data for CaP coatings deposited from biphasic targets and targets of pure HA and TCP are presented in Fig. 3. The coatings were annealed at 700 °C prior to the GIXRD experiment to obtain more intense peaks from the coating material. As shown by the GIXRD analysis, the HA is the dominant phase for all coatings deposited from targets of different composition. Crystal planes (211), (112), (002), (300) and (202) have been registered in all the deposited coatings. With the decrease in the TCP content in the targets, the peak intensities related to HA became more pronounced. The TiO_2 phase formation due to the high-temperature annealing and substrate oxidation is present in all the coatings. Moreover, the CaO phase also appears in all the coatings. According to the GIXRD data, the HA, CaO and TiO_2 peaks intensity is weak, but well-defined. The weak peak intensities are connected to the small coating thickness. No peaks associated to the TCP phase were detected. From this, after annealing, the coatings consist of the HA phase alone. However, an overlap of the TCP peaks with those of the HA may take place. The presence of CaO phase in all the sputtered coatings might be caused by annealing. According to [20], annealing in the air leads to decomposition of calcium phosphates with the CaO formation according to the equation:

$$Ca_{10}(PO_4)_6(OH)_2 \rightarrow 3Ca_3(PO_4)_2 + CaO + H_2O. \qquad (1)$$
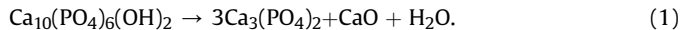
It has been shown that HA decomposition may occur at relatively low (900 °C) annealing temperature, instead of 1150–1200 °C, as mentioned in some papers [21]. It has also been noted that annealing of the CaP coatings on Ti substrates leads to Ti oxidation. The oxygen for oxidation is supposedly taken from the coating material.

XRD spectra of all five types of depleted targets are presented in Fig. 4. It is important to note that in all the cases, CaO diffraction peaks are absent is the spectra. The phase composition of the biphasic targets correlates well with the mixture ratios of HA and TCP. In the case of the 75HA/25TCP target, the amount of the TCP phase is small. Solitary peaks of TCP are found in the range of $2\Theta = 36°–41°$. Where the angles of the TCP and HA diffraction maximums overlap, the HA peaks are slightly increased. The TCP phase is predominant in the spectra related to the 50HA/50TCP and 25HA/75TCP targets. The CaO formation is related to either the RF magnetron sputtering or the annealing step but is not connected to the target sintering procedure. Certain ion species are known [22] to be present in the plasma during sputtering, namely: CaO^+, Ca^{2+}, PHO^+, PO^+, P^+, PO_4^{3-}. These species condense on the substrate
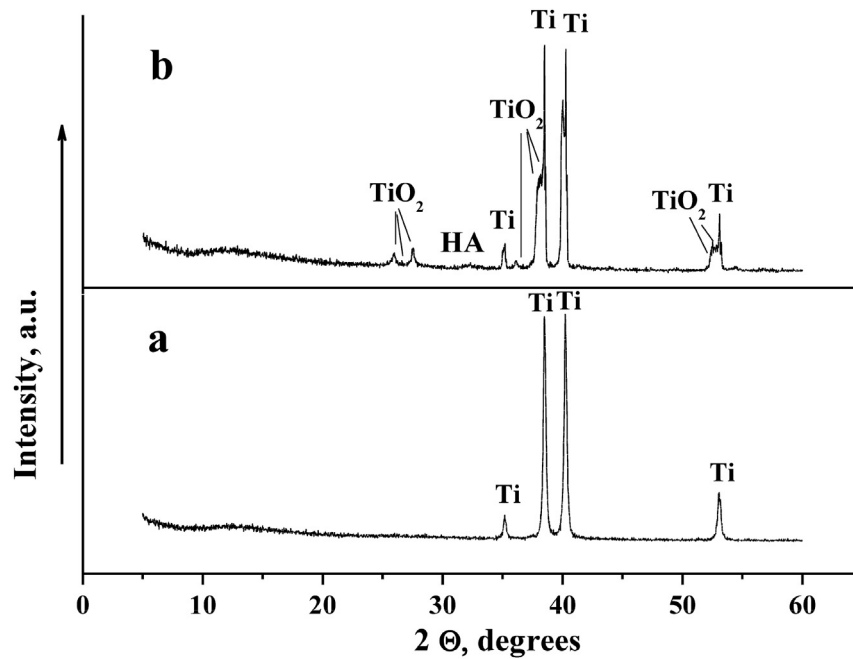
Fig. 2. XRD pattern of the CaP coatings on the Ti substrates after the sputtering process (a) and after the annealing at 700 °C for 1 h (b).
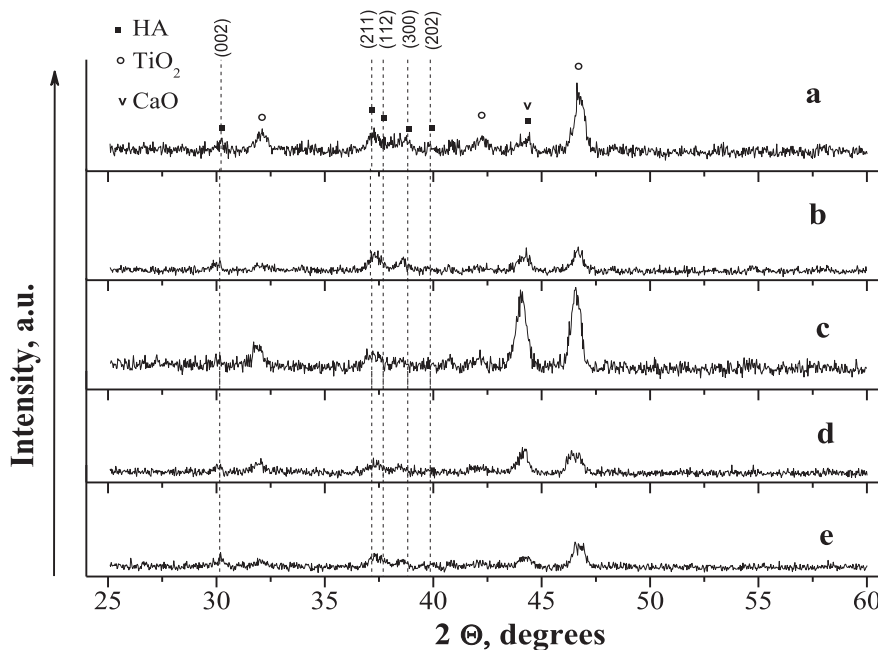

Fig. 3. The diffractograms obtained in grazing angle geometry from thin coatings deposited from the following targets: 100HA (a), 75HA/25TCP (b), 50HA/50TCP (c), 25HA/75TCP (d) and 100TCP (e).

as ad-atoms, subsequently, forming the coating structure. One of the sputtered ion groups is CaO, which in the coating and forms a separate CaO phase.

In case of sputtering of biphasic targets, the EDX analysis of the coatings shows an increase in the Ca content, which can be associated to the increased amount of the CaO phase in such coatings. Thus, one can conclude that the content of Ca and CaO is increased in the coatings sputtered from biphasic targets [23]. According to the EDX data, the increased TCP content in the biphasic targets causes deviation in the elemental composition of the films. A correlation between the Ca/P ratio of the biphasic coatings and the TCP concentration in the targets is revealed in Fig. 5. From the plot, it is seen that the Ca concentration is increased with the increase of the TCP content in the biphasic targets. After sputtering, the biphasic targets become sub-stoichiometric as the concentration of Ca decreases, correlating with the increase of the Ca amount in the coatings.

After a series of sputtering, the Ca content in the biphasic targets is decreased proportionally to the increased Ca content in the sputtered coatings. In the case of the 25HA/75TCP biphasic target,
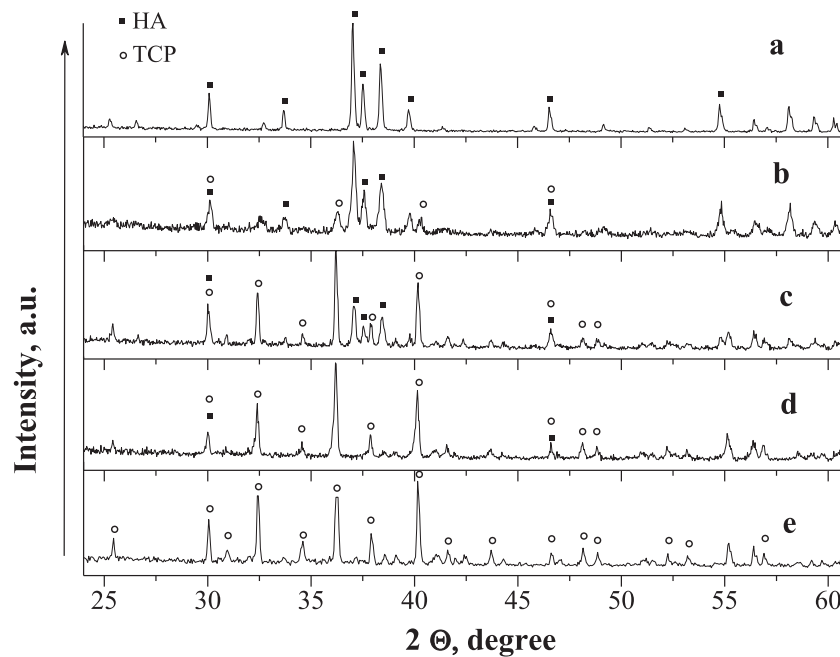
Fig. 4. The diffractograms obtained from the following targets: 100HA (a), 75HA/25TCP (b), 50HA/50TCP (c), 25HA/75TCP (d) and 100TCP (e).

the Ca/P ratio is equal to 0.8. As a result, the target became Ca deficient compared to the original composition. However, with the increased HA content in the 75HA/25TCP target, the Ca/P ratio was increased up to 1.26, while an inverse situation is observed in the coatings. The Ca/P ratio in the coating deposited from the 25HA/75TCP biphasic target is equal to 2.54, so that Ca is intensively sputtered from the TCP rich target. It is also known, that CaO is the most weakly bonded component in the HA and is actively sputtered from TCP rich targets [23]. The binding energy of the CaO molecule is 91 kcal/mol, whereas for the PO_4^{3-} group it is 142 kcal/mol. As such, the sputtering of CaO is expected to prevail, and the concentration of Ca in the coating is expected to increase.

In Table 1, the theoretical Ca/P ratio is compared with the EDX data for the targets and for the as-deposited coatings. The
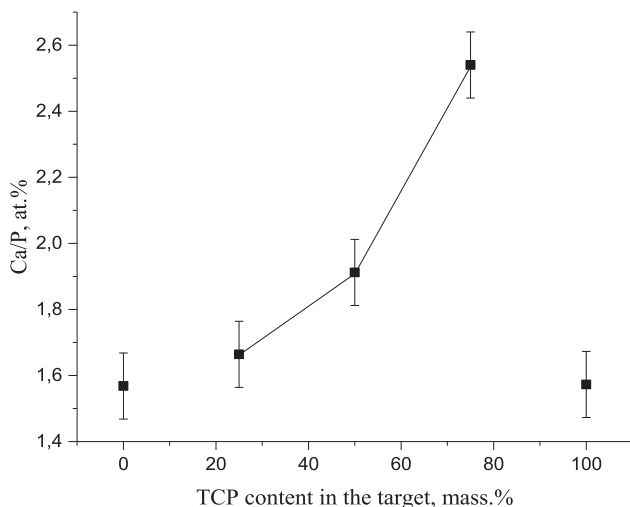
calculated atomic ratio of Ca/P = 1.52 for the 25HA/75TCP biphasic target is quite far from the experimental value of Ca/P = 2.54 in the coating which reveals a stark difference between the theoretical and experimental Ca/P content in both the coatings and the targets of the biphasic materials. On the other hand, the EDX data of pure HA and TCP targets and coatings compare favourably with theoretical values. From this, one can conclude that sputtering process of the biphasic targets of homogeneous mixtures of HA and TCP powders of different ratios is selective because CaO^+ and Ca^{2+} more actively sputtered from the targets. In the case of sputtering of pure HA or TCP targets, this effect is not pronounced, if it exists. Thus, it is possible to manipulate the Ca/P ratio in the coatings by varying the content of HA and TCP components in biphasic targets.

Raman-spectra of all five types of as-deposited coatings on Ti substrates are presented in Fig. 6. Symmetric vibration mode of PO_4^{3-} (v_1) in the 920-980 cm^{-1} range has its maximum intensity in the HA spectrum. In the 200-800 cm^{-1} range, the TiO_2 bands of high intensity are present, which overlap with the CaP bands. After annealing (see Fig. 7), in the 1000-1200 cm^{-1} range, the Raman shifts characteristic for PO_4^{3-} (v_3) vibration apatite mode become visible. Peak intensities of PO_4^{3-} (v_1) are higher for the annealed samples as compared to the as-deposited ones. This same trend is observed for the TiO_2 region. Change in TiO_2 vibration modes' intensity is connected to the annealing. During the high temperature treatment, the thicker oxide layer is formed. Moreover, recrystallization of the coating takes place after annealing. This can be concluded from the fact that PO_4^{3-} (v_3) vibration mode appeared in the spectra. The Raman spectroscopy results for the annealed samples are in correspond well with the GIXRD spectra.

4. Conclusions

Thin quasi-amorphous CaP coatings on Ti substrates can be obtained by RF magnetron sputtering of biphasic targets consisting of homogeneous mixtures of HA and TCP in different proportions as well as of single HA and TCP targets. The structure, composition and morphology of the coatings can be controlled by the biphasic


Fig. 5. Ca/P ratio in the thin coatings deposited from the biphasic targets versus TCP content.

Table 1
Theoretical and experimental Ca/P ratio for biphasic targets and as-deposited coatings.

Type of the target	HA/TCP mass ratio	Estimated ratio of Ca/P	Ca/P ratio in the coatings	Ca/P ratio in the targets
HA100	HA	1,67	1,57 ± 0,2	1,4 ± 0,2
HA75/TCP25	3/1	1,58	1,66 ± 0,2	1,26 ± 0,2
HA50/TCP50	1/1	1,54	1,91 ± 0,2	0,95 ± 0,2
HA25/TCP75	1/3	1,52	2,54 ± 0,2	0,81 ± 0,2
TCP100	TCP	1,5	1,57 ± 0,2	1,38 ± 0,2
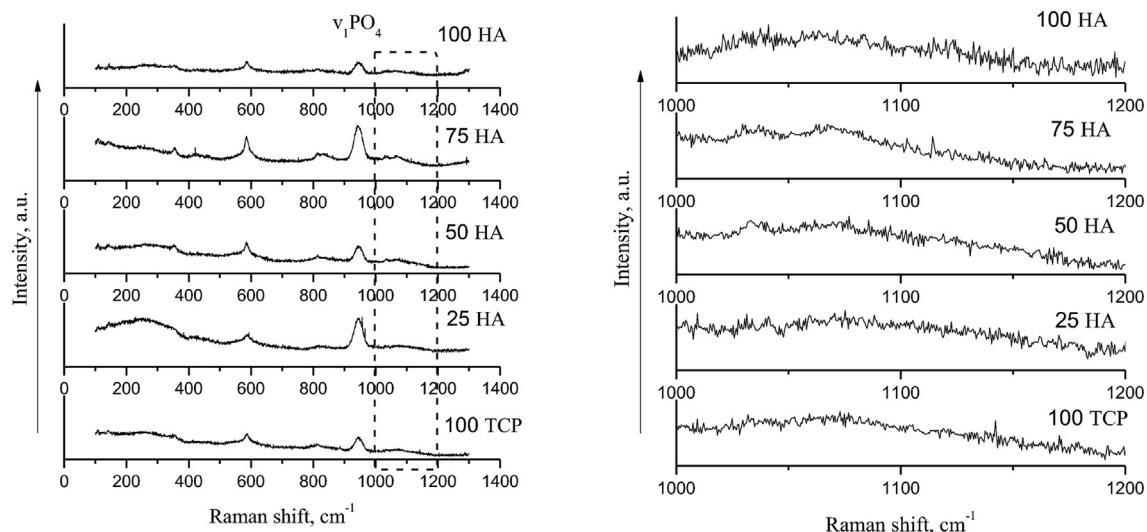
Fig. 6. Raman spectra from as-deposited coatings from the following targets: 100HA (a), 75HA/25TCP (b), 50HA/50TCP (c), 25HA/75TCP (d) and 100TCP (e).
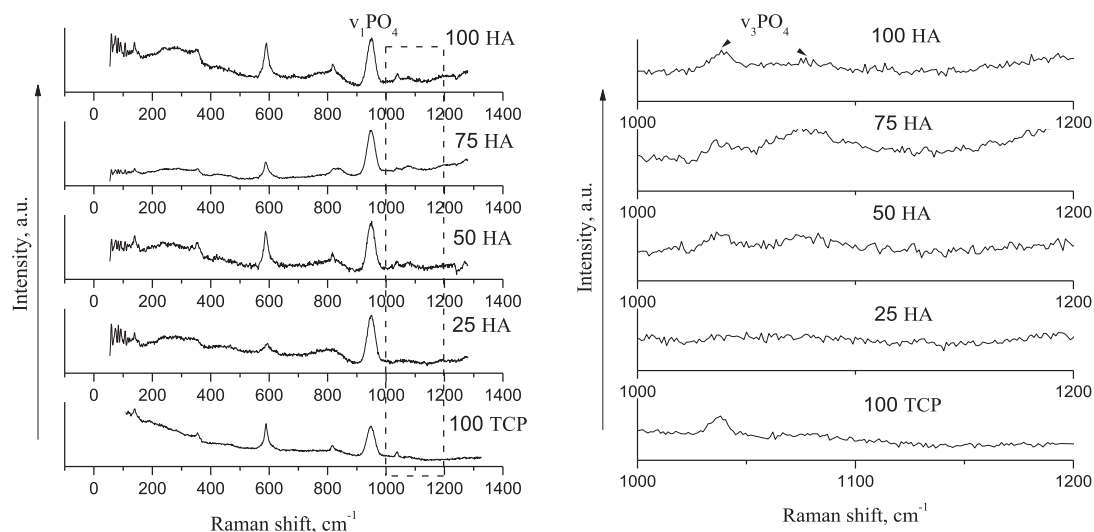
Fig. 7. Raman spectra from coatings deposited from targets after annealing: 100HA (a), 75HA/25TCP (b), 50HA/50TCP (c), 25HA/75TCP (d) and 100TCP (e).

targets composition. The increase in the TCP proportion in the target mixture leads to the decrease of the average size of the surface structural elements to its minimum (about 78 nm in the case of single-phase TCP target). According to the GIXRD data, single-phase HA coatings are formed after annealing. Depletion in the Ca content of the biphasic targets in connection with the number of sputtering cycles, revealed by the EDX, is correlated with the increase in the TCP content. The Ca content in the coatings increases in the same proportion and can be used to tailor the elemental composition of the coatings.

Acknowledgements

References

[1] W. Cao, L.L. Hench, Bioactive materials, Ceram. Int. 22 (1996) 493–507, http://dx.doi.org/10.1016/0272-8842(95)00126-3.

[2] B.D. Ratner, A.S. Hoffman, Physicochemical surface modification of materials used in medicine, in: Biomater. Sci. An Introd. to Mater, third ed., 2013, pp. 259–275, http://dx.doi.org/10.1016/B978-0-08-087780-8.00027-9.

[3] R.B. Heimann, Structure, properties, and biomedical performance of osteo-conductive bioceramic coatings, Surf. Coatings Technol. 233 (2013) 27–38, http://dx.doi.org/10.1016/j.surfcoat.2012.11.013.

[4] A. Ogose, T. Hotta, H. Kawashima, N. Kondo, W. Gu, T. Kamura, N. Endo, Comparison of hydroxyapatite and beta tricalcium phosphate as bone sub-stitutes after excision of bone tumors, J. Biomed. Mater. Res. - Part B Appl. Biomater. 72 (2005) 94–101, http://dx.doi.org/10.1002/jbm.b.30136.

[5] G.E. Stan, D.A. Marcov, I. Pasuk, F. Miculescu, S. Pina, D.U. Tulyaganov, J.M.F. Ferreira, Bioactive glass thin films deposited by magnetron sputtering technique: the role of working pressure, Appl. Surf. Sci. 256 (2010) 7102–7110, http://dx.doi.org/10.1016/j.apsusc.2010.05.035.

[6] R.A. Surmenev, A review of plasma-assisted methods for calcium phosphate-based coatings fabrication, Surf. Coatings Technol. 206 (2012) 2035–2056, http://dx.doi.org/10.1016/j.surfcoat.2011.11.002.

[7] I. Mutreja, D. Kumar, A.R. Boyd, B.J. Meenan, Titania nanotube porosity con-trols dissolution rate of sputter deposited calcium phosphate (CaP) thin film coatings, RSC Adv. 3 (2013) 11263, http://dx.doi.org/10.1039/c3ra40898a.

[8] J.G.C. Wolke, J.P.C.M. Van Der Waerden, H.G. Schaeken, J.A. Jansen, In vivo dissolution behavior of various RF magnetron-sputtered Ca-P coatings on roughened titanium implants, Biomaterials 24 (2003) 2623–2629, http://dx.doi.org/10.1016/S0142-9612(03)00067-X.

[9] A.R. Boyd, G.A. Burke, H. Duffy, M. Holmberg, C. O'Kane, B.J. Meenan, P. Kingshott, Sputter deposited bioceramic coatings: surface characterisation and initial protein adsorption studies using surface-MALDI-MS, J. Mater. Sci. Mater. Med. 22 (2011) 74–84, http://dx.doi.org/10.1007/s10856-010-4180-8.

[10] K. Ozeki, J.M. Janurudin, H. Aoki, Y. Fukui, Photocatalytic hydroxyapatite/ti-tanium dioxide multilayer thin film deposited onto glass using an rf magne-tron sputtering technique, Appl. Surf. Sci. 253 (2007) 3397–3401, http://dx.doi.org/10.1016/j.apsusc.2006.07.030.

[11] J.S. Suwandi, R.E.M. Toes, T. Nikolic, B.O. Roep, Inducing tissue specific toler-ance in autoimmune disease with tolerogenic dendritic cells, Clin. Exp. Rheumatol. 33 (2015) 97–103, http://dx.doi.org/10.1002/jbm.a.

[12] Y. Yonggang, J.G.C. Wolke, L. Yubao, J.A. Jansen, The influence of discharge power and heat treatment on calcium phosphate coatings prepared by RF magnetron sputtering deposition, J. Mater. Sci. Mater. Med. 18 (2007) 1061–1069, http://dx.doi.org/10.1007/s10856-007-0119-0.

[13] M.V. Chaikina, V.F. Pichugin, M.A. Surmeneva, R.A. Surmenev, Mechano-chemical synthesis of hydroxyapatite with substitutions for depositing the coatings on medical implants by means of high-frequency magnetron sput-tering, Chem. Sustain. Dev. 17 (2009) 507–513.

[14] A.A. Ivanova, R.A. Surmenev, M.A. Surmeneva, T. Mukhametkaliyev, K. Loza, O. Prymak, M. Epple, Hybrid biocomposite with a tunable antibacterial activity and bioactivity based on RF magnetron sputter deposited coating and silver nanoparticles, Appl. Surf. Sci. 329 (2015) 212–218, http://dx.doi.org/10.1016/j.apsusc.2014.12.153.

[15] M. Ebrahimi, M.G. Botelho, S.V. Dorozhkin, Biphasic calcium phosphates bio-ceramics (HA/TCP): concept, physicochemical properties and the impact of standardization of study protocols in biomaterials research, Mater. Sci. Eng. C 71 (2017) 1293–1312, http://dx.doi.org/10.1016/j.msec.2016.11.039.

[16] T.L. Arinzeh, T. Tran, J. Mcalary, G. Daculsi, A comparative study of biphasic calcium phosphate ceramics for human mesenchymal stem-cell-induced bone formation, Biomaterials 26 (2005) 3631–3638, http://dx.doi.org/10.1016/j.biomaterials.2004.09.035.

[17] M.B. Sedelnikova, Y.P. Sharkeev, E.G. Komarova, I.A. Khlusov, V.V. Chebodaeva, Structure and properties of the wollastonite???calcium phosphate coatings deposited on titanium and titanium???niobium alloy using microarc oxida-tion method, Surf. Coatings Technol. 307 (2016) 1274–1283, http://dx.doi.org/10.1016/j.surfcoat.2016.08.062.

[18] S.V. Dorozhkin, Nanodimensional and nanocrystalline hydroxyapatite and other calcium orthophosphates, Am. J. Biomed. Eng. 1 (2013) 1–90, http://dx.doi.org/10.3390/ma2041975.

[19] D.O. Costa, P.D.H. Prowse, T. Chrones, S.M. Sims, D.W. Hamilton, A.S. Rizkalla, S.J. Dixon, The differential regulation of osteoblast and osteoclast activity by surface topography of hydroxyapatite coatings, Biomaterials 34 (2013) 7215–7226, http://dx.doi.org/10.1016/j.biomaterials.2013.06.014.

[20] M.O. Takayoshi Nakano, Kazuhiro Kaibara, Yukichi Umakoshi, Satoshi Imazato, Koretada Ogata, Atsushi Ehara, Shigeyuki Ebisu, Change in microstructure and solubility improvement of HAp ceramics by heat-treatment in a vacuum, Mater. Trans. 43 (2002) 3105–3111, http://dx.doi.org/10.2320/matertrans.43.3105.

[21] A.Y. Berezhnaya, V.O. Mittova, A.V. Kostyuchenko, I.Y. Mittova, Solid-phase interaction in the hydroxyapatite/titanium heterostructures upon high-temperature annealing in air and argon, Inorg. Mater. 44 (2009) 1214–1217, http://dx.doi.org/10.1134/S0020168508110137.

[22] S. Xu, J. Long, L. Sim, C.H. Diong, K. Ostrikov, RF plasma sputtering deposition of hydroxyapatite bioceramics: synthesis, performance, and biocompatibility, Plasma Process. Polym. 2 (2005) 373–390, http://dx.doi.org/10.1002/ppap.200400094.

[23] K. Mediaswanti, C. Wen, E. P, C.C. Berndt, J. Wang, Sputtered hydroxyapatite nanocoatings on novel titanium alloys for biomedical applications, in: Titan. Alloy. - Adv. Prop. Control, InTech, 2013, http://dx.doi.org/10.5772/54263.